

Spatiotemporal Changes in Ocular Morphology and White Matter Integrity in a Transgenic Mouse Model of Chronic Glaucoma

Xiao-Ling Yang^{1,2}, Leon C. Ho^{1,3}, Yolandi van der Merwe^{1,4}, Ian P. Conner^{2,4}, Seong-Gi Kim^{1,5}, Gadi Wollstein², Joel S. Schuman^{2,4}, and Kevin C. Chan^{1,2}

¹NeuroImaging Laboratory, University of Pittsburgh, Pittsburgh, Pennsylvania, United States, ²Department of Ophthalmology, School of Medicine, University of Pittsburgh, Pittsburgh, Pennsylvania, United States, ³Department of Electrical and Electronic Engineering, The University of Hong Kong, Pokfulam, Hong Kong, China, ⁴Department of Bioengineering, Swanson School of Engineering, University of Pittsburgh, Pittsburgh, Pennsylvania, United States, ⁵Center for Neuroscience Imaging Research, Institute for Basic Science, Sungkyunkwan University, Suwon, Korea

Target Audience: Scientists and clinicians interested in understanding the etiology and progression of glaucoma as a neurodegenerative disease of the visual system.

Purpose: Glaucoma is the leading cause of irreversible blindness in the world and is a slowly progressing neurodegenerative disease of the eye and the brain. While elevated intraocular pressure (IOP) and age are the common risk factors, the underlying pathogenesis of glaucoma is still uncertain. Uncovering the full spatiotemporal profile of glaucoma in the visual system is important for determining the etiology and pathophysiological events of the disease and for making targeted therapeutic strategy. In this study, we evaluated longitudinally the IOP, ocular anatomy and brain microstructural integrity with an aim to probe the onset of glaucomatous changes and their progression in a transgenic mouse model of chronic glaucoma using DBA/2J (D2) mice. In addition, age-matched C57BL/6J (B6) mice were used as a control to study the effect of age on the eye and the brain. Visuomotor function was assessed by the end of the experimental period to determine the final visual outcome in both groups of animals.

Methods: Animal Preparation: Thirteen D2 and 6 B6 female mice underwent longitudinal anatomical T2-weighted imaging (T2WI) of the eye and diffusion tensor imaging (DTI) of the brain at 5, 7, 9 and 12 months old (m.o.) (n=4 for B6 at 9 and 12 m.o.). The IOP of both eyes were measured every 1-2 months using the TonoLab rebound tonometer (Fig. 1). An OptoMotry virtual reality system (CerebralMechanics Inc.) was used to assess the visuomotor behavior by quantifying the visual acuity of each eye of both D2 and B6 mice at 12 m.o. **MRI Protocols:** All MRI experiments were performed under isoflurane anaesthesia using a 9.4-Tesla/31-cm Varian/Agilent scanner with a 32mm transmit-receive volume coil. For anatomical ocular MRI, T2-weighted imaging (T2WI) was acquired using a fast spin echo sequence with TR/TE=2000/42.4, ETL=8, NEX=20, FOV=14x14mm², MTX=192 and slice thickness=0.5mm. Slices were oriented to bisect the center of both eyes. DTI was acquired using a fast spin echo sequence, with 12 diffusion gradient directions at b=1.0ms/μm² and 2 non-diffusion-weighted images at b=0ms/μm² (b₀). Other imaging parameters included: TR/TE= 2300/27.8ms, ETL=8, δ/Δ=5/17ms, NEX=4, FOV=2.0x2.0cm², acquisition matrix= 192x192 (zero-filled to 256x256), and slice thickness= 0.5mm. Slices were oriented orthogonal to the prechiasmatic optic nerves. **Data Analysis:** For anatomical T2WI, several ocular dimensions [anterior chamber depth (ACD), vitreous body depth (VBD) and axial length (AL)] were measured in each eye using ImageJ (Fig. 2). DTI parametric maps including fractional anisotropy (FA), axial diffusivity (λ_a) and radial diffusivity (λ_r) were computed using DTIStudio. Regions of interest were manually drawn on the prechiasmatic optic nerve and optic tract based on FA, λ_a and λ_r maps and the mouse brain atlas using ImageJ (Figs. 3 and 4). IOP, ocular dimensions, DTI parametric values and visual acuity were compared between D2 and B6 using two-tailed unpaired t-tests. Comparisons among time points were performed using one-way ANOVA followed by post-hoc Tukey's tests.

Results: IOP (Fig. 1): The IOPs of D2 mice began to increase at 8-9 m.o., reached its peak at 10 m.o. and remained significantly higher than 5 m.o. till the end of experimental period. Interestingly, a small but significant increase in IOP was also observed in B6 mice at 9 m.o. onward; **Ocular morphology (Fig. 2):** All 3 ocular dimensions (ACD, VBD and AL) significantly increased in D2 mice as IOP began to increase at 9 m.o.. The ACD and AL continued to increase in D2 mice as IOP rose further after 9 m.o.. B6 mice also showed a slight increase in AL but at 7 m.o. without further enlargement afterwards; **White matter microstructure (Figs. 3 and 4):** FA, λ_a and λ_r changes began at 9 m.o. in the optic nerve at D2 and progressed further at 12 m.o.. A smaller extent of DTI changes was observed in the optic tract of D2 at 9 and 12 m.o.. In B6 group, a small but significant λ_r decrease was observed in the optic nerve at 9 and 12 m.o.; **Visuomotor function:** At 12 m.o., the visual acuity of D2 mice (0.035±0.060 cycle/degree) was significantly worse than that of B6 (0.380±0.026 cycle/degree) (p<0.001).

Discussion and Conclusions: The spatiotemporal profiles of IOP, ocular morphology and white matter integrity in D2 and B6 mice were characterized. The ocular dimensions and microstructures of visual pathway in D2 mice began to change at the onset of IOP increase at 8-9 m.o. and progressed further at 12 m.o., resulting in significant deterioration in visuomotor function compared to B6 mice of the same age. As IOP and λ_r also altered slightly in aged B6 compared to younger B6 mice, cautions should be taken when employing B6 as an age-matched negative control to D2 for glaucoma studies.

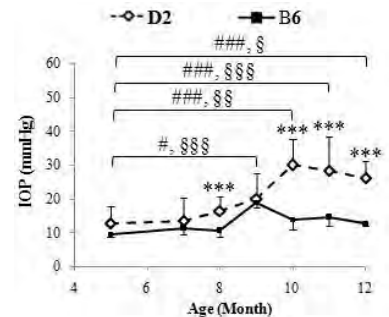


Fig. 1: Intraocular pressure (IOP) profiles of D2 and B6 mice from 5 to 12 months old. (Two-tailed unpaired t-tests between D2 and B6: ***p<0.001; post-hoc Tukey's test between 5 m.o. and other time points, D2: #p<0.05, ##p<0.01; B6: \$p<0.05, \$\$p<0.01, \$\$\$p<0.001; comparisons among other time points are not shown here for clarity)

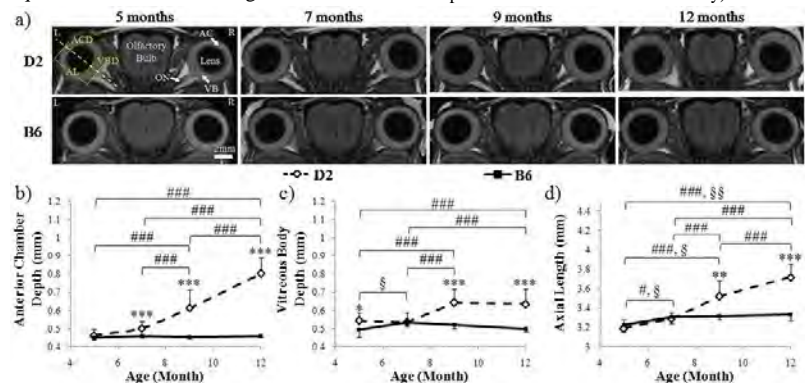


Fig. 2: Anatomical T2-weighted MRI of ocular dimensions [anterior chamber depth (ACD), vitreous body depth (VBD) and axial length (AL)] in D2 and B6 mice across time. (Two-tailed unpaired t-tests between D2 and B6: *p<0.05, **p<0.01, ***p<0.001; post-hoc Tukey's tests among all time points, D2: ###p<0.001; B6: \$p<0.05, \$\$p<0.01) (ON: Optic Nerve; AC: Anterior Chamber; VB: Vitreous Body)

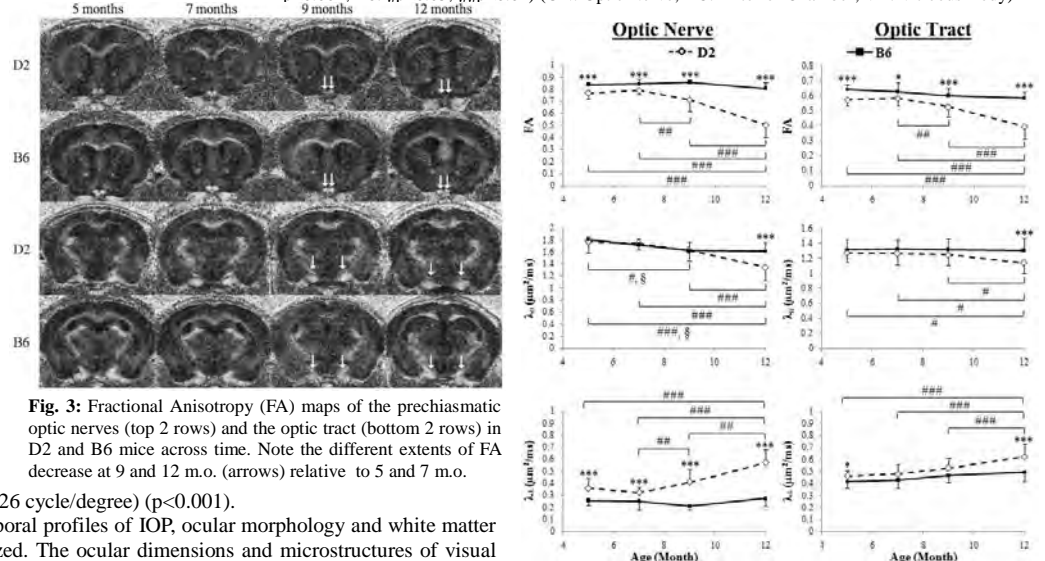


Fig. 3: Fractional Anisotropy (FA) maps of the prechiasmatic optic nerves (top 2 rows) and the optic tract (bottom 2 rows) in D2 and B6 mice across time. Note the different extents of FA decrease at 9 and 12 m.o. (arrows) relative to 5 and 7 m.o.

Fig. 4: Quantitative spatiotemporal DTI profiles of optic nerve and optic tract in D2 and B6 mice (Two-tailed unpaired t-tests between D2 and B6: *p<0.05, **p<0.01, ***p<0.001; post-hoc Tukey's tests among all time points, D2: #p<0.05, ##p<0.01, ###p<0.001; B6: \$p<0.05).